

# Effect of an electric field on the magnetization processes in the yttrium iron garnet $\text{Y}_3\text{Fe}_5\text{O}_{12}$

B. B. Krichevskov, R. V. Pisarev, and A. G. Selitskiy

*A. F. Ioffe Physicotechnical Institute, USSR Academy of Sciences, St. Petersburg*

(Submitted 26 August 1991)

Zh. Eksp. Teor. Fiz. **101**, 1056–1072 (March 1992)

We investigate the influence of electric and magnetic fields on the magnetization process in cubic ferromagnets, the yttrium iron garnets  $\text{Y}_3\text{Fe}_{5-x}\text{Ga}_x\text{O}_{12}$  (where  $x = 0$  and  $0.6$ ). The polarimetric method we have developed allowed us to investigate the magnetic structure at a local resolution of  $\sim 2.5 \mu\text{m}$  within individual domains and in regions containing individual domain walls. Using this experimental setup, we were able to find the true value of the magnetoelectric susceptibility in various magnetization regimes for the first time. We observed that at normal magnetization of a thin film the magnetoelectric (ME) effect is observed in individual domains even in a zero magnetic field, remaining unchanged up to fields at which a transition occurs to a regime in which the magnetization vector is free to rotate; furthermore, its value is considerably larger than previously reported for investigations involving averaging methods. Our theoretical analysis shows that the ME effect in individual domains is proportional to the ratio  $E^2/K_1$ , where  $E$  is the applied electric field and  $K_1$  is the first magnetic anisotropy constant. In the regime where the magnetization vector can rotate, the magnetoelectric effect is determined by the ratio  $E^2/4\pi M_s^2$ , where  $M_s$  is the spontaneous magnetization, and is considerably smaller than in individual domains. We establish that the electric field can cause translation of domain walls when a magnetic field is present. When the film is magnetized parallel to its plane, the ME effect in the domain increases with increasing field within the range  $0 < H < H_A$ , where  $H_A$  is the anisotropy field, and has a singularity at  $H \approx H_A$ . We show that this effect is connected with the absence of demagnetizing fields in this geometry.

## 1. INTRODUCTION

A change in the magnetic state of a crystal under the action of an electric field is one of a number of physical phenomena that are collectively referred to as “magnetoelectricity” and whose existence is due to a coupling between the electric and magnetic fields in matter.<sup>1,2</sup> Depending on the experimental conditions, the magnetoelectric (ME) effect is manifest either as a change in the magnetization  $\mathbf{M}$  of a sample under the action of an external electric field  $\mathbf{E}$ , or as the appearance of an electric polarization under the action of the magnetic field  $\mathbf{H}$ , or accompanying a spontaneous magnetization  $\mathbf{M}$ . In view of this, both inductive and capacitive methods can be used to observe the ME effect; descriptions of several of these methods can be found in Ref. 3. In recent times, the ME effect has also been investigated using optical polarimetric methods, which are based on recording a rotation of the polarization plane of light (the Faraday effect) as the magnetization changes under the action of an electric field.<sup>4–7</sup>

Over the course of many years, yttrium iron garnet  $\text{Y}_3\text{Fe}_5\text{O}_{12}$  (YIG) has always been a model system in the physics of magnetic phenomena.<sup>8</sup> The ME effect in this cubic ferrimagnet was observed for the first time in Ref. 9, and was subsequently studied in a number of other papers.<sup>5,10–13</sup> These investigations showed that the ME effect in YIG is quadratic in the electric field, is absent for  $H = 0$ , is odd with respect to the magnetic field  $H$ , and is observed in a limited range of magnetic fields  $H < H_s$ , where  $H_s$  is the saturation field. The ME susceptibility obtained in these experiments has a value on the order of  $\beta^{\text{ME}} \approx 10^{-6}$  in Gaussian units. An effect that is linear in the electric field was recently ob-

served in YIG crystals cooled in external fields.<sup>14,15</sup> Analysis of the experimental data reveals that the primary mechanism by which an electric field  $E$  affects the magnetization of iron garnets is by changing the magnetic anisotropy of the crystal.<sup>13,16</sup> Apparently this mechanism is also decisive in other magnetically ordered crystals with spontaneous magnetization, e.g., in magnetite  $\text{Fe}_3\text{O}_4$  (Ref. 17) or in the lithium spinel  $\text{LiFe}_5\text{O}_8$  (Ref. 18). The influence of the electric field on the magnetization of the sample can manifest itself differently in various regimes; therefore in investigations of specific mechanisms for the ME effect in garnets several hypotheses have been advanced, which connect the nature of this effect either with changes in the magnetization within individual domains,<sup>10</sup> or with processes that rotate the magnetization,<sup>13</sup> or with motion of domain walls in an electric field.<sup>6</sup> Reliable tests of the validity of these or other hypotheses have been hampered, in our opinion, by the fact that the experimental methods used up to now (inductive and capacitive) do not have the spatial resolution required for observing the ME effect within single magnetic domains or within individual domain walls.

It is important to note that the magnetoelectric susceptibility  $\beta^{\text{ME}}$  measured in averaging experiments by inductive and capacitive methods can in principle differ considerably from the ME susceptibility of an individual domain or region containing a domain wall, since the measured signal is averaged over a large number of different domains and domain walls. The situation is complicated further by the fact that when no domain structure is present, e.g., in the regime where the magnetization can rotate or in saturation, the ME susceptibility can also differ significantly from the value of

$\beta^{\text{ME}}$  within a domain. Thus, whereas the spontaneous magnetization of a domain can be determined by measuring the magnetization of a saturated sample, the situation is entirely different for the case of magnetization caused by the ME effect, because there is no ME effect in a saturated sample.

In our view, this problem can be resolved by using optical polarimetric methods, which allow us to record the rotation of the plane of polarization of light in external electric and magnetic fields (i.e., the electromagnetooptic (EMO) effect).<sup>5,6</sup> To be sure, preliminary investigations of the EMO effect in YIG, which were carried out with insufficiently high spatial resolution, showed that the EMO effect in this crystal, in contrast, e.g., to  $\text{Cr}_2\text{O}_3$  (Ref. 6), is almost completely determined by the action of the electric field on the magnetization of the sample, while the contribution associated with the change of the magneto-optic susceptibility in an electric field is very small.<sup>5</sup> Thus, the EMO effect in iron garnets may be considered to be an optical analog of the ME effect.

The goal of this study was to investigate experimentally the influence of an electric field on the magnetic structure of yttrium iron garnet in various regimes of magnetization with a spatial resolution sufficient to study individual magnetic domains and domain walls. This has allowed us to determine the true ME susceptibility and reveal the mechanism by which an electric field affects the magnetization processes in YIG. As far as we know, investigations of this type have never been carried out before.

## 2. EXPERIMENTAL SETUP

The experimental setup consists of a combination of a laser polarimeter<sup>4-6</sup> and a polarization microscope. In Fig. 1 we show the optical part of the setup. Linearly polarized laser radiation that has passed through the polarizer 1 is focused by the objective 2 into a region with a diameter between 5 and 50  $\mu\text{m}$  on the crystal 3. Radiation passing through the crystal falls on the objective of microscope 5, and is split by a half-silvered mirror 7 into two beams. The beam reflected from the mirror is used to monitor the domain structure visually, using the polarizer 8, the vidicon 9, and the video monitoring apparatus 10. The linear scale of the image of the domain structure obtained on the television

screen, was calibrated using an object micrometer and case to 0.8  $\mu\text{m}/\text{mm}$ . The resolving power of the microscope was  $\approx 0.7 \mu\text{m}$ . The radiation passing through the splitter 7 was used to measure the rotation of the plane of polarization of light in the sample under the action of the electric and magnetic fields (the EMO effect).

In order to investigate individual sections of the crystal, a region was cut out of the optical image formed by the objective 5 using a circular iris 6 of diameter 0.30 mm; this region corresponded to sections of the crystal of diameter 2.5  $\mu\text{m}$ . By displacing the iris in two mutually perpendicular directions, we were able to choose various regions of the crystal and carry out measurements of the effect as a function of the iris position. The threshold sensitivity of the polarimeter when a single-mode laser LG-52-1 was used, with radiated power 16 mW, depended on the diameter of the focused spot, and ranged in a recording band of  $\sim 1 \text{ Hz}$  from  $2.4 \cdot 10^{-6}$  up to  $7 \cdot 10^{-6} \text{ rad}$ . The apparatus allowed us to simultaneously measure either the magnitude of the EMO effect  $\delta\alpha^{\text{EMO}}$  and the Faraday effect (FE)  $\alpha_F$ , or the magneto-optic susceptibility  $\chi_{\text{MO}}$  and the FE, as functions of the constant magnetic field  $H$  (0 to 1.2 kOe) (0 to  $10^5 \text{ A/m}$ ) produced by an electromagnet, or as a function of the coordinates  $x$  and  $y$  that define the position of the iris 6.

In order to investigate the EMO effect, the polished surface of the crystal was covered by platinum or gold semi-transparent electrodes 4 to which we applied an AC electric field with  $\omega = 700 \text{ Hz}$  such that  $U_- = 500 \text{ V}$ . The measurement of  $\delta\alpha^{\text{EMO}}$  was made at the second harmonic  $2\omega$  of the applied field, since the EMO in garnets is quadratic in the electric field. In order to create a weak AC magnetic field  $h_-$  of strength  $\sim 1 \text{ Oe}$  ( $80 \text{ A/m}$ ), we used several coils placed on the electromagnetic cores. The measurement of  $\chi_{\text{MO}} = \partial\alpha_F/\partial h_-$  was carried out at the first harmonic  $\omega$  of the AC magnetic field  $h_-$ .

We studied the single-crystal yttrium iron garnet (YIG)  $\text{Y}_3\text{Fe}_5\text{O}_{12}$  and the yttrium gallium iron garnet  $\text{Y}_3\text{Fe}_{4.4}\text{Ga}_{0.6}\text{O}_{12}$  (YGIG). The samples were slabs with area  $4 \times 5 \text{ mm}$  and thickness  $\sim 50 \mu\text{m}$ , cut along (100) planes. The characteristic width of a domain at  $H = 0$  was about 10  $\mu\text{m}$  for YIG and about 25  $\mu\text{m}$  for YGIG. The measurements were carried out in the geometries  $\mathbf{K} \parallel \mathbf{H} \parallel \mathbf{E} \parallel \mathbf{h}_-$  and  $\mathbf{K} \parallel \mathbf{E} \perp \mathbf{H}$  for  $T = 295 \text{ K}$ .

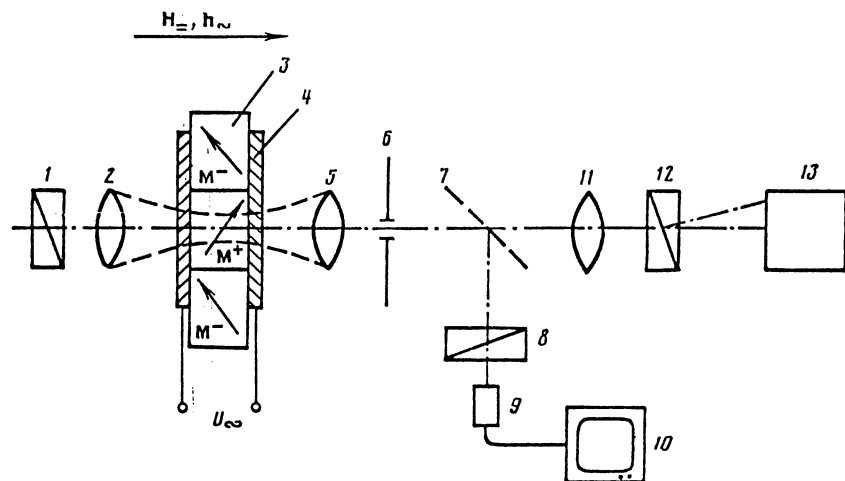


FIG. 1. Optical portion of the polarimeter for investigation rotation of the polarization plane of light in electric and magnetic fields with a local resolution of 2.5  $\mu\text{m}$ . (1)—polarizer, (2,5,11)—objectives, (3)—crystal under study, (4)—semitransparent electrodes, (6)—circular iris, (7)—semitransparent mirror, (8–12)—optical analyzer, (9)—vidicon, (10)—video control apparatus, (13)—differential photodetector.

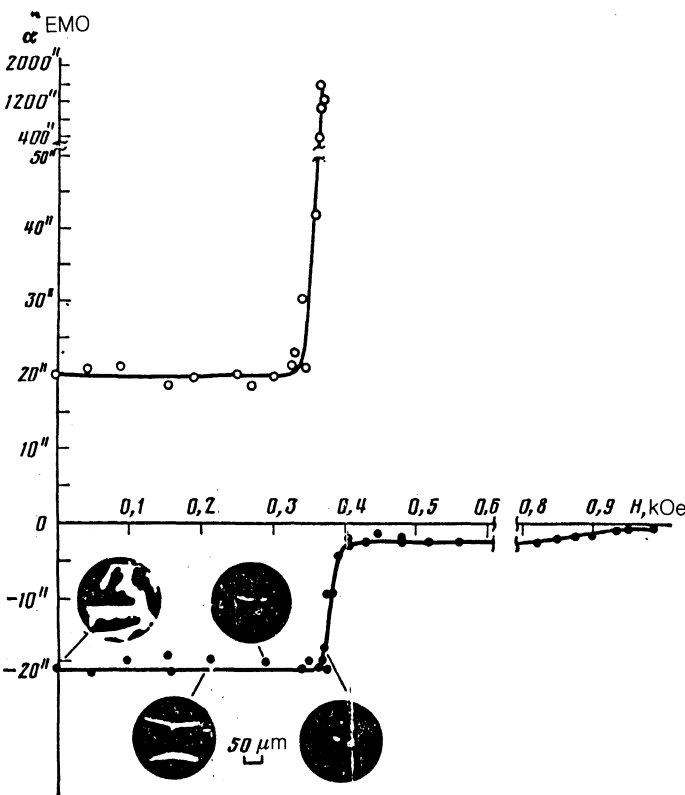


FIG. 2. Field dependence of the angle of rotation  $\delta\alpha^{\text{EMO}}$  of the polarization plane of the light induced by an electric field  $E_z = 10^7 \text{ V/m}$  in YGIG within individual magnetic domains  $M^+$  (●) and  $M^-$  (○) for normal magnetization;  $\mathbf{k} \parallel \mathbf{H} \parallel \mathbf{E}$ , with  $\mathbf{k} \parallel [100]$ ,  $\lambda = 0.633 \mu\text{m}$ . Also shown is the typical form of a domain structure for specific values of the magnetic field in the regime of domain-wall motion.

### 3. EXPERIMENTAL RESULTS

The results of previous investigations of the EMO effect in YIG with a resolution of  $\sim 150 \mu\text{m}$  (Ref. 5) showed that there is no  $\delta\alpha^{\text{EMO}}$  when  $H = 0$ , nor the ME effect,<sup>9,11-13</sup> and that  $\delta\alpha^{\text{EMO}}$  depends linearly on  $H$  in the regime of domain-wall motion. The picture we observed when we measured  $\delta\alpha^{\text{EMO}}$  for individual magnetic domains was fundamentally different. In Fig. 2 we show the field dependence of  $\delta\alpha^{\text{EMO}}$  for normal magnetization of the slab in the central portions of individual “positive” domains (i.e., domains  $M^+$  for which  $\mathbf{M} \cdot \mathbf{H} > 0$ ) and “negative” domains (i.e., domains  $M^-$  for which  $\mathbf{M} \cdot \mathbf{H} < 0$ ) in a YGIG crystal. The terms “positive” (“negative”) characterize domains whose volume increases (decreases) as the magnetic field  $H$  increases. The measurements in this case were carried out in such a way that the regions investigated did not contain domain walls.

The figure shows also photographs of the domain structure for various values of the field  $H$ .

In zero magnetic field we observed a rotation of the plane of polarization of the light  $\delta\alpha^{\text{EMO}}$  that was quadratic in the field  $E$ , with a value  $\sim 20''$  for  $E = 10^7 \text{ V/m}$ . In a YIG crystal (see Fig. 3) under the same conditions the corresponding value of  $\delta\alpha^{\text{EMO}}$  was  $10''$ . In domains characterized by different signs of the projection of the magnetization  $\mathbf{M}$  onto the direction of propagation of the light  $\mathbf{k}$  (the white and black domains shown in Fig. 2), the sign of the EMO effect was different, while the magnitude of the effect was the same. This circumstance explains the absence of an ME effect in zero field when measured by averaging methods.<sup>6,9,11-13</sup> As the magnetic field  $H$  increased into the range 0–340 Oe corresponding to the regime of domain-wall motion, in contrast to the results of averaging measurements

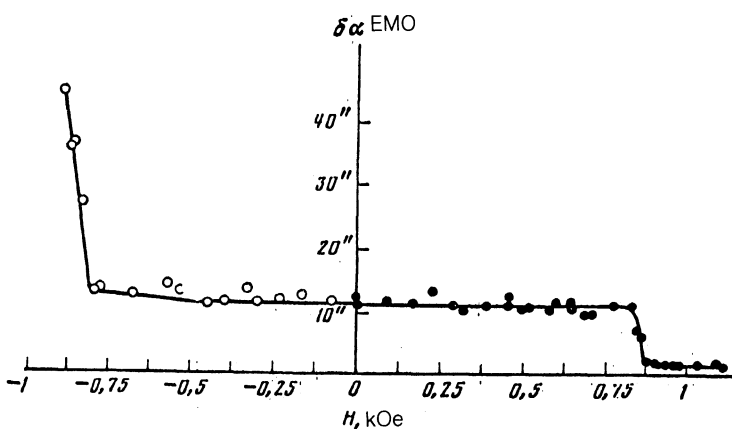


FIG. 3. Field dependence of the angle of rotation  $\delta\alpha^{\text{EMO}}$  of the polarization of the light induced by an electric field  $E = 10^7 \text{ V/m}$  in YIG within an individual magnetic domain for two opposite directions of the magnetic field  $H$ , with  $\mathbf{k} \parallel \mathbf{H} \parallel \mathbf{E}$  with  $\mathbf{k} \parallel [100]$ . By definition, changing the direction of the magnetic field transforms a  $M^+$  (●) domain into a  $M^-$  (○) domain.

where a linear increase in  $\delta\alpha^{\text{EMO}}$  was observed, the EMO effect for positive and negative domains remained constant.

As we pass into the region where the magnetization can rotate, in YGIG ( $H \gtrsim 390$  Oe) the quantity  $\delta\alpha^{\text{EMO}}$  decreases rapidly in a positive domain  $M^+$  to a value (1 to 2) $''$ , and then falls to a residual value  $\approx 0.3''$  at  $H \gtrsim 1$  kOe. In a domain  $M^-$  we observe a very rapid growth in the EMO effect in this region of fields up to values  $\sim 1600''$ . Further increase of the field causes the negative  $M^-$  domains to collapse. An analogous behavior of the EMO effect is also observed in the YIG  $\text{Y}_3\text{Fe}_5\text{O}_{12}$  (Fig. 3). It follows from the definition given above that an  $M^+$  domain turns into an  $M^-$  domain when the sign of the magnetic field changes.

When a YIG slab is magnetized in the plane  $\mathbf{H} \perp \mathbf{k}$ , the behavior of the ME effect in an individual domain differs considerably from the case of normal magnetization. In the range of fields  $H = 0$  to 69 Oe,  $\delta\alpha^{\text{EMO}}$  increases, and the growth of the signal accelerates rapidly as  $H_A$  is approached (Fig. 4). In fields  $H \approx 68.5$  Oe the value of  $\delta\alpha^{\text{EMO}}$  is more than an order of magnitude larger than in the absence of a magnetic field. For  $H > 69$  Oe, i.e., when we enter the saturation regime, the electric field ceases to affect the magnetization.

Let us now consider the action of an electric field on a region of the crystal containing a domain wall (DW), for normal magnetization  $\mathbf{H} \parallel \mathbf{k}$ . In Fig. 5 we show plots of  $\delta\alpha^{\text{EMO}}$  and the FE when the iris is scanned over crystal seg-

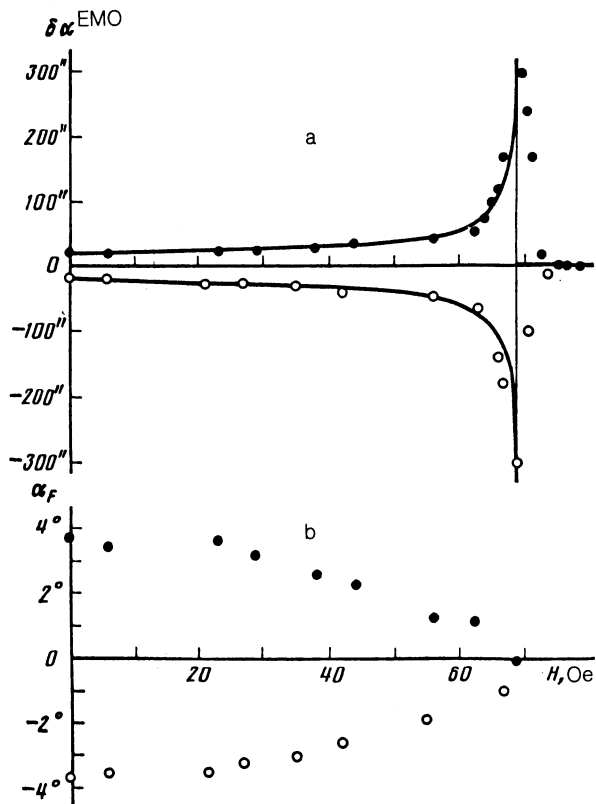


FIG. 4. Field dependence of the angle of rotation  $\delta\alpha^{\text{EMO}}$  of the polarization plane of the light induced by an electric field  $E = 10^7$  V/m in YIG within an individual magnetic domain (a) and the FE effect in the domain (b) for the case of a magnetic field in the plane, i.e.,  $\mathbf{k} \parallel \mathbf{H} \perp \mathbf{E}$ ; here  $\mathbf{k} \parallel [100]$ . The points are experimental, the curves theoretical.

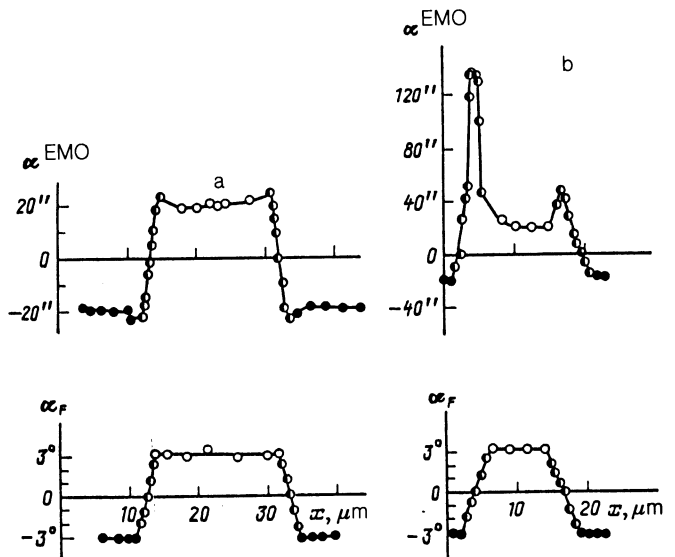


FIG. 5. Dependence of the magnetooptic ( $\alpha_F$ , lower curve) and electromagnetooptic ( $\delta\alpha^{\text{EMO}}$ , upper curve) rotations of the plane of polarization of light in YGIG as a function of the iris position as it moves from one domain to another: (a)  $H = 0$ , (b)  $H = 300$  Oe; The points corresponding to the EP transversion in 0, determine the position of the domain limits at  $x$  axes. ●— $M^+$ , ○— $M^-$  domain.

ments containing a domain wall for  $H = 0$  (a) and  $H = 300$  Oe (b). For  $H = 0$  the dependences of  $\delta\alpha^{\text{EMO}}$  and of the FE on the coordinate  $x$  of the iris are identical. As we go from an  $M^+$  domain to an  $M^-$  domain, the values of  $\delta\alpha^{\text{EMO}}$  and  $\alpha_F$  change sign. The point of intersection with the  $x$  axis corresponds to the case where the domain wall is located in the middle of the region under study, where the contribution to  $\alpha_F$  and  $\delta\alpha^{\text{EMO}}$  from domains  $M^+$  and  $M^-$  cancel out. For  $H \neq 0$  a sharp peak appears in the functions  $\delta\alpha^{\text{EMO}}(x)$ , corresponding to a position of the DW in the middle of the region under study bordered by the iris (Fig. 4b). The sign of the  $\delta\alpha^{\text{EMO}}$  peaks coincides with the sign of  $\delta\alpha^{\text{EMO}}$  in the negative domain  $M^-$ . The magnitude of  $\delta\alpha^{\text{EMO}}$  at the peak depends on the position of the domain wall in the crystal, on the shape of the magnetic domain, and on the magnetic field  $H$ . As Fig. 4b shows, the peaks of  $\delta\alpha^{\text{EMO}}$  can differ significantly in magnitude even for adjacent DW. The values of the peaks averaged over several DW increase linearly with increasing magnetic field  $H$ .

It is clear from Fig. 2 that the domain structure of the crystal changes in a magnetic field  $H$  of around 280 Oe. In these fields the stripe domains  $M^-$  are disrupted and elliptical domains are formed and decrease in area as the magnetic field is decreased further, and their shape becomes cylindrical. In fields  $H \approx 390$  Oe the residual  $M^-$  domains collapse, and in stronger fields we enter a regime where the magnetization can rotate. In Fig. 6 we show the distribution of  $\delta\alpha^{\text{EMO}}$  for an individual  $M^-$  domain of elliptical shape at  $H = 340$  Oe when the iris is scanned along the directions  $A-A$  and  $B-B$ . In this figure we also show the magnetooptic susceptibility as a function of coordinates  $x$  and  $y$ . The largest values of  $\delta\alpha^{\text{EMO}}$  are observed for wall segments with maximum curvature (cross section  $A-A$ ). On these segments of the DW we also observe maxima of the local dynamic

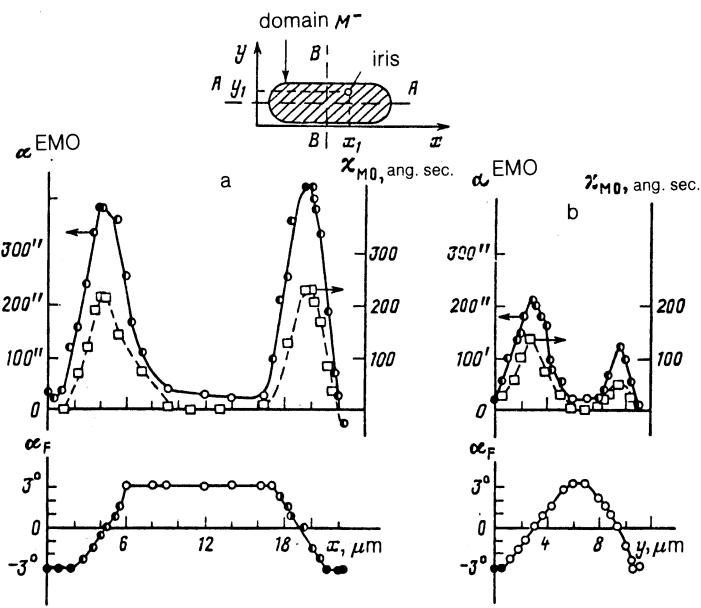


FIG. 6. Dependence of the magneto-optic rotation  $\alpha_F$  and electro-magneto-optic rotation  $\delta\alpha_{EMO}$  of the plane of polarization of light as a function of the iris position in domain of elliptic shape. (a)— $A-A$  is a scan along the major axis  $x$  ( $y = 7 \mu\text{m}$ ). (b)— $B-B$  is a scan along the minor axis  $y$  ( $x = 15 \mu\text{m}$ ). The squares show the corresponding magnetooptical susceptibility. The external field  $H = 340$  Oe; ● is for  $M^+$ , and ○ for  $M^-$  domains.

magnetooptical susceptibility  $\chi_{MO}$ ; however, in contrast to  $\delta\alpha_{EMO}$  within a domain, the magnitude of  $\chi_{MO}$  reduces to zero. Thus, the EMO and ME effects in segments that contain a DW depend on the curvature of the DW; specifically, these effects decrease with increasing radius of curvature.

No motion of the domain walls was observed for transverse magnetization.

#### 4. THEORETICAL DESCRIPTION AND DISCUSSION OF RESULTS

##### 4.1. Phenomenological description of how the field $E$ affects the magnetic anisotropy of cubic crystals

The magnetic anisotropy of a cubic crystal of class  $m3m$  is described by terms of the type

$$W_A = K_{ijkl} \alpha_i \alpha_j \alpha_k \alpha_l, \quad (1)$$

where  $\alpha_i$  are the direction cosines of the magnetization and  $K_{ijkl}$  is a fourth-rank tensor that is symmetric with respect to all its indices and has two nonzero coefficients  $K_{11}$  and  $K_{23}$ . In this case  $K_1 = K_{23} - 2K_{11}$ , where  $K_1$  is the first anisotropy constant of a cubic magnet. Terms that are sixth order in the magnetization, which are described by a second constant  $K_2$ , are not considered here. The change in the anisotropy energy  $\delta W_A(E)$  caused by an electric field  $E$  can be expressed by the relation

$$\delta W_A(E) = E^2 R_{ijkl} \beta_i \beta_j \alpha_k \alpha_l, \quad (2)$$

where  $\beta_i$  and  $\beta_j$  are direction cosines of the electric field and  $R_{ijkl}$  is a fourth-rank tensor symmetric in all pairs of indices which in the class  $m3m$  under discussion has three independent coefficients  $R_{11}$ ,  $R_{12}$ , and  $R_{44}$ . With regard to its symmetry properties, this tensor is analogous to the magnetostriction and magnetic birefringence tensors.<sup>19</sup> It is meaningful to include in the anisotropy energy  $W_A$  only those terms that ensure its angular dependence; therefore, in practice the number of independent phenomenological coefficients necessary to describe  $W_A$  reduces to three. In invariant form the anisotropy energy of a cubic crystal in a field  $E$  can be written in the form<sup>16</sup>

$$W_A = K_1 (\alpha_1^2 \alpha_2^2 + \dots) + CE^2 (\alpha_1^2 \beta_1^2 + \dots) + DE^2 (\alpha_1 \alpha_2 \beta_1 \beta_2 + \dots), \quad (3)$$

where  $C = R_{11} - R_{12}$ ,  $D = R_{44}$ , and the symbol  $\dots$  denotes a cyclic permutation of the indices 1, 2, 3. The axes 1, 2, 3 coincide with the fourfold axes of the crystal. The contribution of various invariants to  $W_A$  is determined by the direction of the electric field. For example, when the electric field is oriented along the fourfold axis [100],  $\beta_2 = \beta_3 = 0$ ,  $\beta_1 = 1$ , and the change in the anisotropy is determined only by the coefficient  $C$ . In other cases, there are contributions from both coefficients  $C$  and  $D$ .

##### 4.2. Energy of the crystal in the presence of electric and magnetic fields

In its general form, for  $K_1 < 0$  the energy of a cubic magnet having eight types of domain in the presence of electric  $E$  and magnetic  $H$  fields can be written in the following form:

$$W = K_1 \sum_{i=1}^8 V_i (\alpha_{i1}^2 \alpha_{i2}^2 + \dots) + M_S \sum_{ij} V_i \alpha_{ij} H_j + CE^2 \sum_{i=1}^8 V_i (\alpha_{i1}^2 \beta_1^2 + \dots) + DE^2 \sum_{i=1}^8 V_i (\alpha_{i1} \alpha_{i2} \beta_1 \beta_2 + \dots) + N_{jk} M_S^2 \sum_i V_i \alpha_{ij} \sum_i V_i \alpha_{ik} W_I + W_{II} + W_{III} + W_{IV} + W_V, \quad (4)$$

where  $V_i$  is the specific volume of the  $i$ th domain,  $\alpha_{ij}$  are direction cosines on axis  $j$  of the magnetization of the  $i$ th domain, and  $N_{jk}$  is the tensor of demagnetizing coefficients.

The equilibrium values of  $V_i$  and  $\alpha_{ij}$ , which describe the process of magnetization of the crystal, are determined by minimizing  $W$ , and depend in general on the magnitude and direction of the fields  $E$  and  $H$  and on the shape of the sample. The minimization of Eq. (4) with respect to many parameters and samples of arbitrary shape is quite complicated; however, the fundamental regularities can be established

for the special case of magnetization of a thin slab, when  $N_{11} = 2\pi$  while the remaining components of  $N_{ik}$  equal zero.

For  $H = 0$ , the terms  $W_{II}$  and  $W_V$  in (4) are absent, the values of  $V_i$  are the same for all the domains, and the direction of the magnetization in these domains coincides with the direction of the easy-magnetization axis (EMA), which is determined by the minimum of the anisotropy energy in an electric field. In the presence of a magnetic field  $H$ , the terms  $W_{II}$  and  $W_V$  appear in (4) in the regime of domain-wall motion (DWM) ( $V_i \neq 0$ ); however, it turns out that their sum does not depend on  $\alpha_{ij}$ , but rather is only a function of the magnitude of the field, i.e.,  $W_{II} + W_V = f(H^2)$ . As a result, in the DWM regime the directions of the magnetizations  $\alpha_{ij}$  of the domains coincide with the direction of the EMA, which depends on  $E$ , while the independence of the sum of terms  $W_{II} + W_V$  mentioned above is ensured by a corresponding change in the magnitude of  $V_i$ .

When the slab is magnetized in a plane,  $H_2 \neq 0$ , the demagnetizing fields are absent, i.e., the term  $W_V$  equals zero; the parameters  $V_i$  are the same and do not depend on  $E$  and  $H_2$ . The direction cosines  $\alpha_{ij}$  for  $E = E_1$  are determined by minimizing the sum of terms I, II, and III in (4).

In the range where the magnetization can rotate, i.e., when  $H = H_1 > 4\pi M_s / \sqrt{3}$ , we can assume that the crystal contains only a single domain, so that  $V_1 = 1$ ,  $V_{i \neq 1} = 0$ ; however, in contrast to the DWM regime, we must now include all the terms in (4).

#### 4.3. The ME effect in the central region of a domain

Let us consider the case of an ME effect within a domain in the absence of a magnetic field  $H$ . In the geometry we are using ( $E_3 \neq 0$ ,  $E_1 = E_2 = 0$ ), the direction cosines  $\gamma_i$  of the easy-magnetization axis can be found by minimizing (3) under the condition  $\gamma_1^2 + \gamma_2^2 + \gamma_3^2 = 1$ :

$$\begin{aligned}\gamma_1^2 &= 1/3(1+2CE^2/K_1), \quad \Delta\gamma_1(E) = CE^2/3^{1/2}K_1, \\ \gamma_2^2 &= \gamma_3^2 = 1/3(1-CE^2/K_1).\end{aligned}\quad (5)$$

Equations (5) show that for  $K_1 < 0$  the EMA is directed along an axis of type [111] in the absence of an electric field; the field  $E$  causes a deflection of the EMA from this direction into planes of type (110). The EMA deflection direction is determined by the sign of the coefficient  $C$ ; however, it does not depend on the sign of the field  $E$ , by virtue of the quadratic nature of the effect. If  $C > 0$ , then the EMA will deviate in the direction of an axis of type [110], and for  $CE^2 \gg K_1$  the crystal transforms from cubic into a crystal of the easy-plane type (001). For  $C < 0$  the EMA will move in the direction of the [001] axis; i.e., in the "strong field" limit the cubic crystal transforms into a crystal of the "easy axis" type. The magnitude of the deflection of the magnetization is proportional to the ratio  $CE^2/K_1$ ; i.e., the electric field has a stronger effect on the orientation of the magnetization in crystals with small values of  $K_1$ . We can expect that at favorable ratios of the coefficients  $C$ ,  $D$ , and  $K_1$  magnetic orientational transitions can be induced by the electric field.

Starting from the magnitude  $\delta\alpha^{\text{EMO}}$  of the observed effect and the value of  $\alpha_F$  for the FE in an individual domain, we get the ratio  $C/K_1 \approx 1.1 \cdot 10^{-17} \text{ m}^2/\text{V}^2$  for YGIG and  $C/K_1 \approx 2.2 \cdot 10^{-17} \text{ m}^2/\text{V}^2$  for YIG. Since  $K_1$  for YGIG with this composition is roughly half that for YIG, we may conclude that  $C$  is only a weak function of the concentration of

$\text{Ga}^{3+}$  ions. The value of  $C/K_1$  for YGIG corresponds to a rotation of about  $2'$  of the EMA in a field  $E = 10^7 \text{ V/m}$ . We note that in a field  $E = 2 \cdot 10^8 \text{ V/m}$ , according to (5), the change in the direction of the EMA should amount to several degrees. Since the direction of  $\mathbf{M}$  in the domains remains parallel to the EMA in magnetic field ranges corresponding to the regime of domain-wall motion, the EMO and ME effects are constant (Figs. 2, 3).

For the case of a thin slab magnetized in the plane, where  $H = H_2$ , the situation changes considerably. Since there is no net magnetization normal to the surface of the sample, there is no regime of domain-wall motion, and in the range of magnetic fields  $0 < H < H_A$  the magnetization rotates in each domain away from the direction of the easy axis of type [111] toward the direction of the magnetic field  $\mathbf{H}_2$ . The expression for the crystal energy in this case has the form:

$$W = K_1(\alpha_1^2\alpha_2^2 + \dots) + CE_1^2\alpha_1^2 - M_s H_2 \alpha_2. \quad (6)$$

The change in the magnitude of  $\alpha_1$  in fields  $E_1$  and  $H_2$  is described by the expression

$$\Delta\alpha_1 = \frac{CE_1^2}{2^{1/2}K_1} \left[ \frac{1}{2} + \frac{\alpha_2^2}{9\alpha_2^2 - 1} \right] (1 - \alpha_2^2)^{-1/2}, \quad (7)$$

where  $\alpha_2$  is determined from the equation

$$\alpha_2^3 - \frac{1}{3}\alpha_2 + \frac{2}{3}\frac{H}{H_A} = 0. \quad (8)$$

The calculations show that as the magnetic fields increase within the range  $0 < H < H_A$  the magnitude of  $\Delta\alpha_1$  increases from its value at  $H = 0$  [see (5)], and diverges at  $H = H_A$ . A comparison of the experimental and theoretical functions  $\Delta\alpha_1(H_2)$  (Fig. 4) obtained for previously known values of  $C/K_1$  shows that we do not need a more precise theory to describe the effect, i.e.; the customary approximations remain valid.

#### 4.4. Region in which the magnetization can rotate

Let us now consider the regime in which the magnetization can rotate at  $H = H_1$ . In this regime, there are no  $M^-$  domains in the crystal and the equilibrium direction of the magnetization  $\mathbf{M}$  is determined by the actions of the anisotropy of the field, the external magnetic field, and the demagnetizing field. For the case of normal magnetization of a thin film, the crystal energy can be written in the following form:

$$W = K_1(\alpha_1^2\alpha_2^2 + \dots) + CE_1^2\alpha_1^2 - M_s H_1 \alpha_1 + 2\pi M_s^2 \alpha_1^2, \quad (9)$$

where  $M_s$  is the spontaneous magnetization; the term  $2\pi M_s^2 \alpha_1^2$  is the energy of the demagnetizing field. In order to determine the direction of  $\mathbf{M}$  it is necessary to minimize (9) under the condition  $\alpha_1^2 + \alpha_2^2 + \alpha_3^2 = 1$ .

The equation for  $\alpha_1$  has the form

$$\frac{3}{2}H_A \alpha_1^3 - \left( 4\pi M_s + \frac{H_A}{2} + \frac{2CE_1^2}{M_s} \right) \hat{\alpha}_1 + H = 0, \quad (10)$$

where  $H_A = 2K_1/M_s$ . The solution of this equation shows that the change of  $\alpha_1$  in a field  $E_1$  can be approximately written in the form

$$\Delta\alpha_1 = 2CE^2\alpha_1/M_s(4\pi M_s - H_A). \quad (11)$$

Equation (11) shows that in a regime of rotating magnetiza-

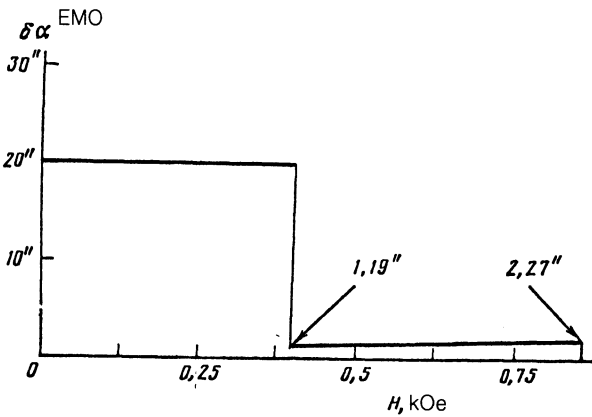


FIG. 7. Calculated field dependence of the electromagnetooptic effect in YIGIG. The jump in rotation in the region of fields  $H \sim 0.38$  kOe corresponds to a transition from a regime of domain-wall motion to a regime of rotating magnetization.

tion the ME effect is determined by the ratio of the anisotropy-energy change in a field  $E$  to the energy of the demagnetizing field, while in the regime of domain-wall motion [see Eq. (5)] the anisotropy energy ( $CE^2/K_1$ ) appears in the denominator. As a consequence of this, as we pass into the region of rotating magnetization, we should expect the magnitude of the ME effect to decrease to a value  $\beta_{H=0}^{ME} H_A / 4\pi M_s$ . In Fig. 7 we show the theoretical field dependence of the EMO effect plotted for a ratio  $C/K_1 = 1.7 \cdot 10^{-17}$  m<sup>2</sup>/V<sup>2</sup>. Comparison (see Fig. 2) of the theoretical and experimental values shows good agreement.

In the range of fields where we pass from the DWM regime to a regime of rotating magnetization, and from the regime of rotating magnetization to the saturation regime, a description of the effect of an electric field on the magnetization direction that is based only on Eq. (4) cannot be sustained. The fact is that the electric field not only acts on the parameters of the magnetic anisotropy, but also changes the values of the critical fields corresponding to transitions from one regime to another. As a result, the magnitude of the ME effect in the transition regions will be determined not only by a quadratic dependence on the electric field, but also by terms of higher order. In this case, we require the inclusion of terms  $\sim E^4$  in the magnetic anisotropy energy for an adequate description of the ME effect and a more precise solution to the equations. The width of the transition region depends on the magnitude of the electric field; in the field range

we have used it is characterized by the value  $\Delta H \approx 0.5$  Oe. Additional smearing of the transition can be due to nonuniformity of the crystal composition, nonuniformity of the magnetization, nonuniformity of the demagnetizing fields, etc.

#### 4.5. The ME effect in samples containing DW

As Figs. 5 and 6 show, an additional ME effect is observed in regions containing DW when  $H \neq 0$  and differs significantly in magnitude from that observed in the central region of the domain. The absence of this effect for  $H = 0$ , and also the fact that the position dependences of  $\delta\alpha^{EMO}$  and the susceptibility  $\chi_M$  in the crystal are the same, attests to the fact that its formation is unconnected with the wall as such, but rather is determined by its motion due to the combined action of the electric and magnetic fields. The mechanism for this DW motion can be clarified in the following way. Application of a magnetic field  $H_1$  to the crystal leads to the appearance of a total magnetization  $M$  in the sample as a consequence of the change in volumes of the  $M^+$  and  $M^-$  domains. In this case the magnetization in the domains is directed along axes of type [111]. We can expect that in the case of unpinned DW the value of  $M_1$  induced by the field  $H_1$  is determined by the expression  $M_1 = H_1 / 4\pi$  and does not depend on the direction of the EMA. The electric field  $E$  leads to rotation of the EMA in the  $M^+$  and  $M^-$  domains. Since the volumes of the domains  $M^+$  and  $M^-$  are different, absence of domain-wall motion should lead to a change in the magnitude of  $M_1$ . Since this is forbidden, changes in the direction of  $M$  in the domains will be offset by a redistribution of the volumes of the domains, i.e., a motion of the domain walls.

Figure 8 shows schematically how the ME and EMO effects are generated by domain walls. Let  $M_1^+$  and  $M_1^-$  denote the projections of the magnetization in the domains  $M^+$  and  $M^-$  along the 1 axis ( $H = H_1$ ,  $E = E_1$ ) while  $\alpha_F$  characterizes the magnitude of the FE. Application of an electric field  $E$  causes a change in the projection  $M_1^+(E) = M_1^+ + \Delta M_1$ , and accordingly a change  $\Delta\alpha_F$  in the FE. In the  $M^-$  domains  $M_1^-(E) = -(M_1^+ + \Delta M_1)$  and  $\alpha_F = (\alpha_F + \Delta\alpha_F)$ . Thus, the ME effect in the domains  $M^\pm$  is determined by the quantities  $\pm \Delta M_1$ , while the EMO effect is determined by the quantities  $\pm \Delta\alpha_F$ . If the change  $\Delta M_1$  is positive, then the volume of the  $M^-$  domain should increase, and the FE or magnetization in the regions containing the DW should change by  $-\Delta\alpha_F$  and  $-\Delta M_1^+$  respectively. Thus, the sign of the EMO (and

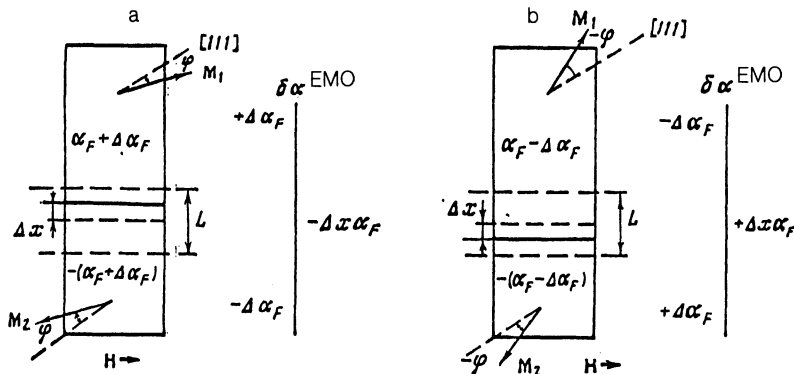


FIG. 8. Schematic illustration of two types of shift  $\Delta x$  of a domain wall into the field of view of the iris ( $L$ ) for rotation of the vectors  $M_1$  and  $M_2$  (domains  $M^+$  and  $M^-$  respectively) under the action of an electric field  $E$  through an angle  $+ \varphi$  (a) or  $- \varphi$  (b) with respect to the EMA [111].

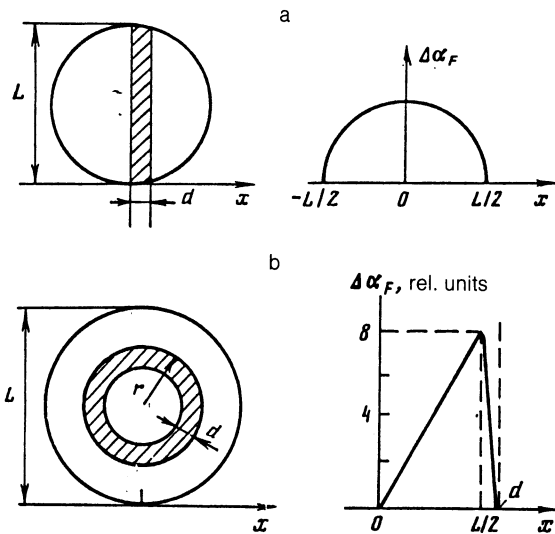


FIG. 9. Geometric model of the appearance of a rotation in the polarization plane of the light under the action of an electric field (the EMO effect,  $\Delta\alpha_F$ ) for the case of motion of planar and annular domain walls within a circular iris.

also the ME) effect from the DW should coincide with the sign of the EMO (ME) effect of a negative domain  $M^-$ , as is in fact observed in experiment. Knowing the magnitude of the Fe in the domains and the diameter of the region of the crystal under discussion, we can estimate, based on the EMO effect, the distance  $\Delta x$  that the DW moves. The calculation shows that the average distance a planar DW moves when  $E = 10^7$  V/m and  $H = 300$  Oe amounts to  $\Delta x \approx 0.01 \mu\text{m}$ .

Investigation of the EMO effect in domains of elliptic shape shows that the magnitude of the effect, and also the magnetooptic susceptibility  $\chi_{\text{MO}}$ , depend on the curvature of the DW. Furthermore, the behavior of  $\delta\alpha^{\text{EMO}}$  and  $\chi_{\text{MO}}$  reflects the fact that the change in volume is due to the change in the length of the planar section of the DW, and is not due to an increase of its curvature, which would require additional energy connected with the surface tension of curved walls.<sup>20</sup>

The anomalous increase of the EMO effect in  $M^-$  domains in fields that are close to the field of collapse (Figs. 2 and 3) is also connected with DW motion. The fact is that the diameter of a  $M^-$  domain in these fields is about 3 to 5  $\mu\text{m}$ ; i.e., it is close to the spatial resolution of our apparatus. Let us analyze the magnitude of the signals that arise in this case within the framework of a simple geometric model (see Fig. 9). Here the change in the size of a domain is determined by the change in its radius  $\Delta r$  or area  $\Delta S$ , while the change in the Faraday effect equals  $\Delta\alpha_F = \alpha_F \Delta S/S$ . If a planar DW (Fig. 8a) moves a distance  $\Delta x$  into the field of view of a circular iris with radius  $r = L/2$ , then the maximum value of the EMO effect is  $\alpha_F \Delta x/L$ . For the case of a cylindrical domain,  $\delta\alpha^{\text{EMO}}$  is determined by the quantity  $\alpha_F 8\Delta r/L$  (Fig. 8b), which for  $\Delta x \approx \Delta r$  is almost an order of magnitude larger than for a planar wall. Thus, the increase in the EMO effect in the precollapsed state is connected with the fact that the radius of the domain becomes comparable to the radius of the region under study.

Let us now analyze the nature of the ME signal measured by integrating-optics, inductance, and capacitance

methods. In these investigations the ME effect in the crystal is not observed when there is no magnetic field  $H$ , despite the fact that domains with oppositely directed magnetizations in and of themselves possess large values of the ME effect, since the volumes of the domains  $M^+$  and  $M^-$  are the same. In the presence of a magnetic field  $H$ , the ME effect is a sum of ME effects of the individual  $M^+$  and  $M^-$  domains, which now have differing volumes, and the ME effect connected with the motion of the DW. If the DW in the crystal were completely free, the ME effect from the domains would be entirely compensated by the motion of the DW. Thus, the linear dependences of  $\delta\alpha^{\text{EMO}}$  on the field observed in regions of DW motion are connected with pinning of the DW by defects, inhomogeneities, etc. Let  $R$  denote the average curvature of the potential well in which a DW is located. Then the potential energy of the DW can be written in the form  $\varepsilon = R(d - d_0)^2$ , where  $d$  is a small reversible displacement with respect to the energetic minimum at  $d_0$ . It is easy to show that the change in the projection of the magnetization  $M_1$ , caused by a change in the direction of the EMA by an amount  $\Delta\varphi$ , can be written in the form

$$\Delta M_1 = -4M_s^2 \mathcal{L} \sin(2\varphi) H \Delta\varphi/R, \quad (12)$$

where  $\mathcal{L}$  is the overall length of the DW. In the case  $R = \infty$ , i.e., when the walls are not pinned,  $\Delta M_1 = 0$ . Thus, the averaged ME effect in the region of DW motion is determined by the degree of pinning of the DW at inhomogeneities and defects. In the region of magnetization rotation, the averaged ME effect has the same value as in the local measurements we have carried out. For normal magnetization it is considerably smaller than the ME effect in individual domains and this decrease is determined by the ratio  $H_A/4\pi M_S$ .

## CONCLUSION

The basic result of this paper is the experimental observation in yttrium iron garnet  $\text{Y}_3\text{Fe}_5\text{O}_{12}$  and yttrium gallium garnet  $\text{Y}_3\text{Fe}_{4.4}\text{Ga}_{0.6}\text{O}_{12}$  of a change in the magnetization within individual magnetic domains that is very large in value under the action of an electric field. The effect is observed even in the absence of a magnetic field, and is connected with changes in the direction of the EMA in an electric field. The magnetolectric susceptibilities in individual domains have the value  $\beta^{\text{ME}} \approx 10^{-5}$ , which exceeds by an order of magnitude the values obtained using averaging methods. The investigation of this effect in various geometries for magnetic fields corresponding to the regime of DW motion and rotation of the magnetization show that the nature of this phenomenon is connected with the presence in the magnetic anisotropy energy of the crystal of terms of the type  $C(\alpha_1^2 E_1^2 + \dots)$ . The magnitude of the ME effect in individual domains for normal magnetization in the region of domain-wall motion is determined by the ratio  $CE^2/K_1$ , and in the region of rotation of the magnetization by  $CE^2/4\pi M_S^2$ . We have determined that the value of  $C/K_1 = 1.1 \cdot 10^{-17} \text{ m}^2/\text{V}^2$  for  $\text{Y}_3\text{Fe}_5\text{O}_{12}$  and  $C/K_1 = 2.17 \times 10^{-17} \text{ m}^2/\text{V}^2$  for  $\text{Y}_3\text{Fe}_{4.4}\text{Ga}_{0.6}\text{O}_{12}$ . For magnetization of the film in its plane we have observed that the ME effect in the domains is singular when  $H \approx H_A$ .

The ME effect connected with the motion of DW was observed in the presence of electric and magnetic fields. De-

pending on the size of the region investigated and the amplitude of DW motion, the effect can reach values that considerably exceed the ME effect in a domain. In studying the ME effect from DW that separate domains of elliptic shape, we observed a dependence of the quantity  $\delta\alpha^{\text{EMO}}$  on the curvature of the DW.

Based on the studies we have made, we have proposed a mechanism that can lead to generation of an ME signal in traditional averaging ME measurements. We show that the existence of an ME effect in the region of DW motion is connected with pinning of the DW by crystal defects.

Based on the general expressions for the energy of a magnet in a magnetic field, with allowance for the effect of the electric field on the magnetic anisotropy, we have developed for the ME effect a theory which describes the change in direction of the magnetization in domains in an electric field. We have obtained for the field dependences of the domain-related ME susceptibilities expressions that describe the experimental dependences quite well, both for the case of normal magnetization and for magnetization in the plane.

In conclusion the authors are grateful to M. V. Krasin'kov for his assistance in depositing the semitransparent electrodes and to T. M. Zhuravlev for polishing the crystals.

<sup>1</sup>L. D. Landau and I. M. Lifshitz, *Electrodynamics of Continuous Media* (in Russian), p. 620, Nauka, Moscow, 1982 [Pergamon, 1984].

- <sup>2</sup>T. H. O'Dell, *The Electrodynamics of Magnetoelectric Media*, p. 304, North-Holland, Amsterdam, 1970.
- <sup>3</sup>*Magnetoelectric Interaction Phenomena in Crystals*, A. F. Freeman and H. Schmid eds., Gordon and Breach, London, N. Y., 1975.
- <sup>4</sup>R. V. Pisarev, B. B. Krichevskov, V. V. Pavlov, and A. G. Selitsky, *J. Magn. Soc. Jpn.* **11** (11), 31 (1987).
- <sup>5</sup>B. B. Krichevskov, R. V. Pisarev, and A. G. Selitskiy, *Fiz. Tverd. Tela (Leningrad)* **30**, 2139 (1988) [Sov. Phys. Solid State **30**, 1233 (1988)].
- <sup>6</sup>B. B. Krichevskov, V. V. Pavlov, and A. G. Selitskiy, *Zh. Eksp. Teor. Fiz.* **94**, 284 (1988) [Sov. Phys. JETP **67**, 378 (1988)].
- <sup>7</sup>B. B. Krichevskov, V. V. Pavlov, and A. G. Selitskiy, *Fiz. Tverd. Tela (Leningrad)* **31**, 77 (1989) [Sov. Phys. Solid State **31**, 1142/1321/2068? (1989)].
- <sup>8</sup>G. Winkler, *Magnetic Garnets*, p. 735, Friedr. Vieweg und Sohn, Braunschweig, 1981.
- <sup>9</sup>T. H. O'Dell, *Phil. Mag.* **16** (141), 487 (1967).
- <sup>10</sup>E. Asher, *Phil. Mag.* **16** (145), 149 (1968).
- <sup>11</sup>M. J. Cardwell, *Phil. Mag.* **20** (167), 1087 (1969).
- <sup>12</sup>G. Velleaud, B. Sangare, and M. Mercier, *JMMM* **31-34**, 865 (1983).
- <sup>13</sup>M. Mercier, *Magnetoelectric Interaction Phenomena in Crystals*, p. 99, A. F. Freeman and H. Schmid (eds), Gordon and Breach, London, N. Y., 1975.
- <sup>14</sup>H. Ogava, E. Kita, Y. Mochida, K. Kohn, S. Kimura, A. Tasaki, and K. Sitatori, *J. Phys. Soc. Jpn.* **56**, 452 (1987).
- <sup>15</sup>E. Kita, K. Sitatori, K. Kohn *et al.*, *J. Appl. Phys.* **64**, 5659 (1988).
- <sup>16</sup>G. Aubert, *JMMM* **31-34**, 767 (1983).
- <sup>17</sup>G. T. Rado and J. M. Ferreri, *Phys. Rev. B* **15**, 290 (1977).
- <sup>18</sup>G. Velleaud, M. Mercier, and G. Aubert, *Solid State Commun.* **44**, 1387 (1982).
- <sup>19</sup>R. V. Pisarev, I. G. Siniy, N. I. Kolpakova, and Yu. M. Yakovlev, *Zh. Eksp. Teor. Fiz.* **60**, 2188 (1971) [Sov. Phys. JETP **33**, 1175 (1971)].
- <sup>20</sup>A. P. Malozemoff and J. C. Slonczewski, *Magnetic Domain Walls in Bubble Materials*, Academic, 1982.

Translated by Frank J. Crowne